Hindawi
Advances in Civil Engineering
Volume 2024, Article ID 1107242, 17 pages
https://doi.org/10.1155/2024/1107242

*Research Article*

# Land Cover and Land Surface Temperature in the West Bank, Palestine

**Ayah Helal and Zahraa Zawawi**

*Urban Planning Engineering, An-Najah National University, Nablus, State of Palestine*

Correspondence should be addressed to Zahraa Zawawi; zahraa.zawawi@najah.edu

Received 16 March 2023; Revised 1 April 2024; Accepted 16 April 2024; Published 30 April 2024

Academic Editor: Daniele Baraldi



The 10 major cities in the West Bank (WB), Palestine—Nablus, Ramallah and Al-Bireh, Jenin, Qalqilia, Salfit, Tubas, Jericho, Bethlehem, Tulkarem, and Hebron—are experiencing rapid urban transformation and changing land cover. This study explores the relationship between land cover (built-up and unbuilt areas) and soil type in these cities across benchmark years 1995, 2000, 2005, 2010, 2015, and 2021. In addition to the former, the paper argues that the expansion and increase of the built-up area and the change in soil type of the aforementioned cities in the West Bank, Palestine, are leading to changes in the land surface temperature (LST). This conclusion was reached through a methodological framework that was developed to measure the relationship between the changing land cover (built-up and unbuilt-up areas), soil type, and LST in the 10 major cities in the region. The framework relies on data retrieved through remote sensing in the years from 1995 to 2021. The results of the analysis conducted through this methodological framework showed that there is an inverse relationship between the increase in built-up areas and LST; however, LST is less inside the built-up areas than in the surrounding areas (open spaces) due to different land cover (unbuilt area with grass and shrubs) and different soil type.

## 1. Introduction

Many studies have been conducted to assess the impact of changing land cover on land surface temperature (LST). ObiefuNa et al. [1], Obiefuna et al. [2], and Kafy et al. [3] argued that the change in land cover is one of the most critical indicators that influence LST. Moreover, the change in the physical properties of the land surface also plays a role in the modification of the LST. This, in turn, points us in the direction that the surface temperatures in rural and agricultural areas are lower than in urban areas. This variation is ascribable to their physical characteristics. These studies will assist both the local government and urban planners in dealing with random expansion, unplanned areas, and urban sprawl, which will help highlight the fact that LST is an urgent issue of the region that should be addressed immediately.

Ayanlade et al.'s [4] research found that the changes in the LULC have greatly influenced the LST in the cities; moreover, the change in land cover and increase of built-up area and the loss of vegetal cover will lead to impervious surfaces resulted in mean monthly and yearly temperature changes. They argued that the core and density areas of cities witnessed higher LST compared with the rural area. Moreover, Maishella et al.'s [5] study aimed to analyze the changes in LC (built-up area) and its relationship with LST in Sleman Regency; results indicated a positive relationship between the increase in the built-up areas and an increase in LST. Ovalle et al. [6] studied the relationship between LULC and LST using the geographical information systems (GIS) and RS in the San Luis Potosí Basin, México. The results showed an opposite relation between vegetation cover density and LST; the less vegetation cover, the higher the LST.

Bindajam et al. [7] argued that densely vegetated land covers have an opposite relationship to the LST and, therefore, lower LST compared to built-up areas. This can be seen in land covers of this nature, the vegetation acts as a preventative measure against incident solar radiation and increases the evaporative cooling effect. This, in turn, lowers the chances of an increase in surface temperature. Moreover, they also claim that the change in LST shows considerable diversions concerning the main aspects linked with elevation, vegetation cover, and solar radiation. He et al. [8] argued that vegetation cover and soil moisture influence LST about topography. It is also noticed that vegetation and LST have an opposite relationship, taking into consideration how the differences in land cover play a role in LST progression due to their different thermal properties [9–11]. Sayão et al. [11] argued that soil has a positive relationship with LST.

The research of Bonafoni and Keeratikasikorn [12] found with the use of field measurements and numerical simulations that both modulation and morphogenesis by cause of active changes in surface characteristics and the presence of urban vegetation can be constructive in modulating the LST, finding that LST has a contrary relationship with increasing the albedo of the built-up surface. It is noted that the same cannot be said for air temperature. Song et al. [9] and Peng et al. [13] found that climate conditions, vegetation, and soil moisture impact LST. They also argued that soil affects vegetation type and vegetative productivity and may be influenced by soil reflectivity, as vegetation and green areas lower LST. Yasir et al. [14] argued that in different climate seasons, vegetation cover changes, where vegetation is more in spring than in autumn, and thus, LST changes accordingly and in opposite relation with vegetation.

Xue et al. [15] found that vegetation feedback and thermal condition showed an inverse relationship among temperature zones. The inverse relationship clarified that vegetation growth can cool most parts of China during climate change. In the end, the pattern of vegetation feedback among land-use types is shown. Due to the expansion of grassland, vegetation feedback may temporarily be positive.

Song et al. [9] argued that green vegetation, especially the ones with big leaves, could efficiently alleviate the urban heat island (UHI) influence by dropping LSTs through evapotranspiration. This will help urban planners and officials understand this relation and how to consider vegetation to lower urban heat. Bindajam et al. [7], Rousta et al. [16], and ObiefuNa et al. [1] found that vegetation lower LST and dense vegetation lower the urban heat, whereas built-up areas increase urban heat. Moreover, built-up areas are warmer than their surroundings and the rural regions; this is because of the concrete and asphalt materials used in the built-up area that increase UHI and LST. Chen et al. [17] argued that UHI is changing according to the changing land use/cover; moreover, the detailed analysis of different types of land use within urban areas indicates that high density of impervious surfaces, population density, and frequent activities of residents play a role in the intensity of UHI. Therefore, the impact of UHI can be mitigated through improved land use planning. Das and Das [18] concluded that by moving from the city center to its surrounding and rural areas with green areas, LST and urban heat phenomenon (UHP) will decrease. This explains that the relationship between built-up areas, LST, and UHP is the opposite. Moreover, they argue that changing LULC impacts LST and UHP as well as the urban greenery and other green areas. This will help urban planners and officials understand this relation and how to consider vegetation to lower urban heat and LST.

Other researchers analyzed the relationship between LST and topography. Peng et al. [13] studied the correlation between the analysis of LST and topographic elements in Hangzhou, China. They found that topography is also a notable characteristic that affects LST. However, its effect on the LST differs depending on the amount of solar radiation acquired, which will have different influences over time. Furthermore, LST is negatively correlated with elevation and slope. He et al. [8] showed a strong inverse relationship between the LST and the elevation for their various study areas.

In the Palestinian context, Aldhshan and Shafri [19] worked on the Gaza Strip by applying GIS and RS techniques to estimate temporal change detection of LULC and LST of the region between 2000 and 2017. They highlighted the relationship between land and demography variations and LST in the same time period. Results indicated a noticeable decrease in the year 2000 and the following 17 years in bare land by 67.19%. This was linked to an increase in urban area (13.12%) due to increased population, crop, and vegetation (4.95%). In addition, they found that the highest temperatures of LST for bare lands are in July and September, which is during summer and autumn, while the lowest is during the winter in January due to the nature of the season and its effects on the area.

Nevertheless, Ghodieh [20] analyzed the change in land cover using RS in the West Bank, Palestine, between the years 1997 and 2016. This analysis was conducted under exceptional and unstable political conditions. He scrutinized inclinations and opportunities for urban expansion in the West Bank and the types of land uses—mainly agricultural and nonagricultural lands. In addition to the latter, his study concluded that most Palestinian urban expansion is an urban sprawl on agricultural lands. Moreover, Raddad [21] inspected and evaluated changes in land use in the Ramallah area. This city, in particular, was chosen due to the noticeable population boom over the past 10 years due to the political conditions in the occupied territories. Satellite images from 1990 to 2003 were used to obtain land use/cover data, and GIS techniques were used to monitor and assess variations in land use during these years. Based on the analysis, it was found that there is a significant relationship between changes in land use and political changes, mostly during unsettled political conditions. This led to informal and swift transformation and the dismantling of areas and natural resources.

However, this paper aims to investigate the correlation between land cover, soil type, and their impact on LST in the West Bank, utilizing Landsat images to examine how these factors are affected by the changing built-up areas within the confined spaces of Palestinian communities. To the researchers' knowledge, this particular investigation has not been previously undertaken. While some studies have utilized Landsat images for land cover assessments in the West Bank, they have yet to research this relationship specifically. The outcomes of this study are anticipated to provide valuable insights for urban planners and policymakers, enabling them to factor in climate change and sustainable development considerations while promoting urban growth. Furthermore, it could serve as a valuable resource in navigating the

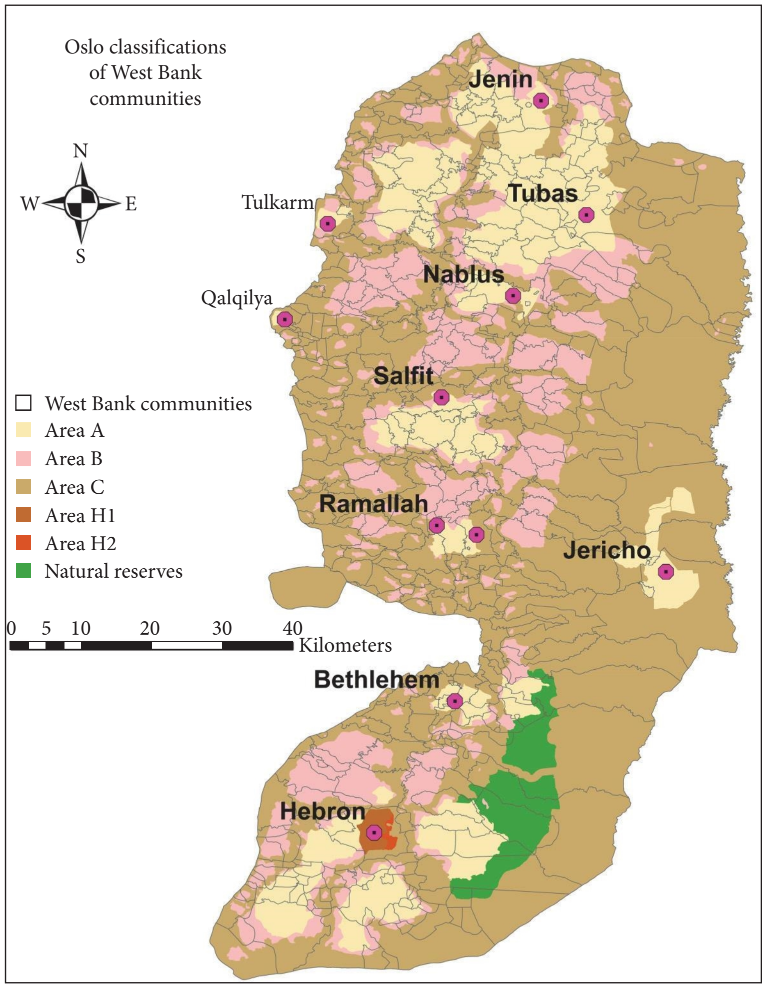


Figure 1: West Bank location (map prepared by researchers, dataset source: MoLG (Ministry of Local Government) [23]).

constraints and policies imposed by the Israeli military occupation, allowing for optimized utilization of the limited areas available for development and discouraging urban sprawl.

## 2. Study Area

There are 3,190,000 [22] Palestinians living in 734 communities (cities, towns, and villages) in the West Bank (Figure 1); the WB was divided into three areas according to the Oslo Interim Agreement of 1995. Area “C” is entirely under the control of the Israeli occupation and covers an area of about 61% of the WB. Area “B” security is under the control of the Israeli occupation; however, its administrative authority is for the Palestinian Authority, and its area constitutes 21% of the WB. Area A falls under the complete administrative and security control of the Palestinian Authority, and its area constitutes 18% of the WB. Hebron “H2” is the area that is administratively subject to Palestinian sovereignty, and “H1” is security-wise subject to the control of the Israeli occupation. This paper selected the 10 major cities to work on due to the high density of their built-up area, large population, and diverse land cover.

## 3. Materials and Methods

In order to assess the effect of the increased built-up area, changing land use, and urban sprawl on the LST in the 10 cities in the WB, this paper developed a methodological framework to measure the relationship between the evolving built-up area, unbuilt area (land cover), and soil type with LST in these particular cities based on the descriptive, analytical, and deductive approaches through quantitative and qualitative evaluation. This was accomplished by using GIS and RS. The methodology of this research went through three steps, as shown in Figure 2.

Step #1: Data collection of various types of datasets:

(i) Landsat images: Landsat 5, 7, and 8 were used to find the LSTs for the years 1995, 2000, 2005, 2010, 2015, and 2021. The source of the images is USGS. Table 1 shows information about the used images. For the years 1995, 2005, and 2010, Landsat 5 TM was used because the images of 2005 and 2010 were not readable by Landsat 7. Band 6 is the thermal band of Landsat 5. For the year 2000, Landsat 7 ETM+ was used, and the bands used were 6.1

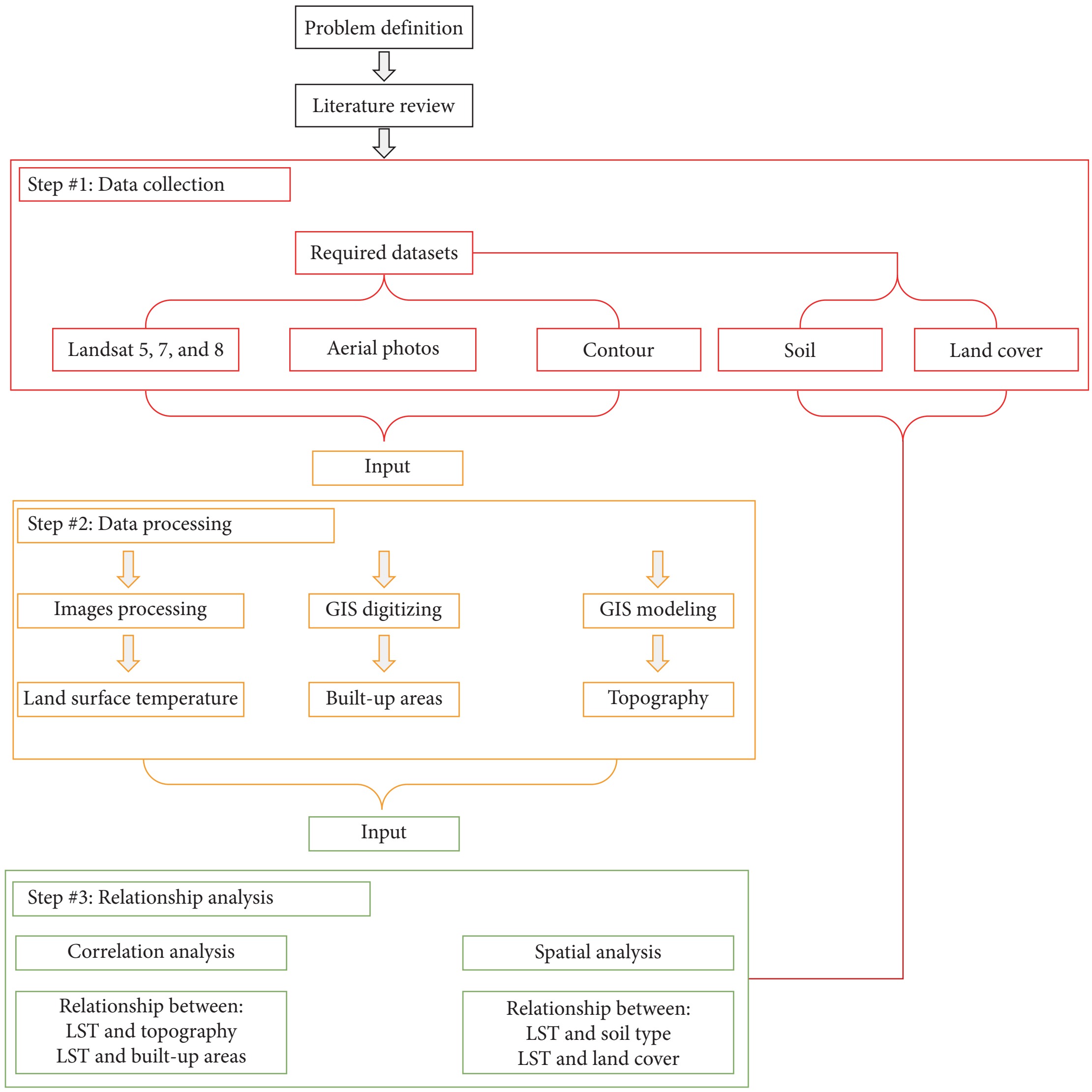


Figure 2: Methodology workflow.

Table 1: Landsat images used in this research with the defined years.

| Landsat based on NDVI | Band | Years |
|---|---|---|
| Landsat 5 TM | 6 | 1995, 2005, 2010 |
| Landsat 7 ETM+ | 6.1, 6.2 | 2000 |
| Landsat 8 TIRS | 10 | 2015, 2021 |

Table 2: Constants used for Landsat 7 and 5 calculations.

| Sensor | Constant 1 (K1) | Constant 2 (K2) |
|---|---|---|
| Landsat 7 ETM+ | 666.09 | 1,282.71 |
| Landsat 5 TM | 607.76 | 1,260.56 |
| Landsat 4 TM | 671.62 | 1,284.30 |

and 6.2. For the years 2015 and 2021, Landsat 8 TIRS (band 10) has been used. It is worth mentioning that the studied month of LST for these years is August (the highest temperature and hottest month in the Palestinian region) to ensure there are no clouds. All Landsat image versions have been studied for the years they are available. Still, the researcher had to use the versions shown in Table 2 due to the availability of clouds in other years for Landsat 8 and 7, which led to using version 5 of Landsat images.

(ii) Aerial photographs have been used to draw the urban areas of the main cities in the West Bank. The source of these photos is the Geomolg website [23]. The electoral communities' boundaries were used to find the unbuilt areas or open spaces within each community's boundaries (Table 3).

(iii) A contour shape file was used to find the topography of the West Bank (Table 3).

Step #2: Data processing: Datasets were processed using GIS (ArcMap). Each dataset has been processed distinctively

TABLE 3: Datasets used in this research with their source and expected output.

| Input | Output | Source |
|---|---|---|
| Landsat | Land surface temperature | [24] |
| Aerial photos | Built-up areas (urban areas) | |
| Contour | Topography | [23] |
| Electoral cities boundaries | To extract open spaces | |

according to its type and the required information. In this step, three substeps have been implemented as follows:

(i) Image processing: The Landsat 5, 7, and 8 has been used to find the LST as follows:

Various algorithms can be used to calculate and find the LST, including the use of single-channel algorithms to recover the LST from the resulting products of Landsat satellites. Similarly, a known substitute, such as images from Landsat satellites, is used to mark changes in LULC. One of the most popular methods of analyzing LST is to use RS. This can also be used to conduct studies on various spatiotemporal domains in a way that the collected information is essential for observing alterations in LULC and LST. This, in turn, establishes an association between the formerly mentioned parameters [6, 25].

GIS has been used to find the LST from the different Landsat images for the West Bank studied years (1995–2005, 2010, 2015, and 2021).

As mentioned in Table 2, different types of Landsat were used each year. For the years 2015 and 2021, Landsat 8 has been used. To find LST from Landsat 8 TIRS, the following steps were applied using a GIS tool, which is the raster calculator.

First, to find the top of atmosphere radiance using the following formula:

$$\mathrm{L}\lambda = \mathrm{ML} \times \mathrm{Qcal} + \mathrm{AL}, \quad (1)$$

where $\mathrm{L}\lambda$ is the TOA spectral radiance, ML is the radiance multiplicative band (3.3420E-04), Al is the radiance add band (0.1), and Qcal is the quantized and calibrated standard product pixel values (DN).

These values are available with each image. They were downloaded from USGS along with the images as a text document.

Second, to find the top of atmosphere brightness temperature using the following formula:

$$\mathrm{BT} = \mathrm{K2}/\ln(\mathrm{K1.L}\lambda + 1) - 273.15, \quad (2)$$

where BT is the top of atmosphere brightness temperature (°C), $\mathrm{L}\lambda$ is the TOA spectral radiance, K1 is the K1 constant band (774.8853), and K2 is the K2 constant band (1321.078). These values are available with each image. They were downloaded from USGS along with the images as a text document.

Third, to find the normalized differential vegetation index (NDVI) using the below formula.

The normalized differential vegetation index (NDVI) is a standardized index for vegetation calculated using near-infrared (Band 5) and red (Band 4) bands. This index is used to find vegetation greenness, which can be used to identify long-term variations of vegetation coverage, which are the main reason for the differences in LST values:

$$\mathrm{NDVI} = (\mathrm{NIR} - \mathrm{RED})/(\mathrm{NIR} + \mathrm{RED}), \quad (3)$$

where RED = DN values from the RED BAND, and NIR = DN values from near-infrared band.

Fourth, to find the land surface emissivity ($E$) using these formulas.

The land surface emissivity (LSE) is the average emissivity of an element of the earth's surface calculated from the NDVI value:

$$\mathrm{PV} = [(\mathrm{NDVI} - \mathrm{NDVImin})/(\mathrm{NDVImax} + \mathrm{NCVImin})]2, \quad (4)$$

where PV is the proportion of vegetation, NDVI is the DN values from NDVI image, NDVImin is the minimum value from NDVI image, and NDVImax is the maximum value from NDVI image.

$$E = 0.004 \times \mathrm{PV} + 0.986, \quad (5)$$

where $E$ is the land surface emissivity and PV is the proportion of vegetation.

Finally, to find the LST using the below formula [26].

The LST is the radioactive temperature which is calculated by using top of atmosphere brightness temperature, land surface emissivity, and the wavelength of emitted radiance:

$$\mathrm{LST} = (\mathrm{BT}/(1 + (\mathrm{W} \times \mathrm{BT}/14,380) \times \ln(E))), \quad (6)$$

where BT is the top of atmosphere brightness temperature (°C), $W$ is the wavelength of emitted radiance, and $E$ is the land surface emissivity [14].

For Landsat 7 and 5, the following procedure is used to find the surface temperature.

First, use band 6 from the image of Landsat 7 and 5 to find the radiance using the following formula:

$$\mathrm{L}\lambda = [(\mathrm{Lmax} - \mathrm{Lmin})/(\mathrm{Qcalmax} - \mathrm{Qcalmin})] \times (\mathrm{Qcal} - \mathrm{Qcalmin}) + \mathrm{Lmin}, \quad (7)$$

where:

L = spectral radiance,

Qcal = quantized calibrated pixel value in DN,

Lmax = spectral radiance scaled to Qcal max = 15.303,

Lmin = spectral radiance scaled to Qcal min = 1.238,

Qcal max = maximum quantized calibrated pixel value = 255, and

Qcal min = minimum quantized calibrated pixel value = 1.

Second, convert the radiance into BT using the following formula. This formula provides the BT in Kelvin (Table 2):

$$\mathrm{BT} = T = \mathrm{K2}/(\ln(\mathrm{K1}/L\lambda + 1)), \quad (8)$$

where:

$T$ = effective at-satellite temperature in Kelvin,

K2 = calibration constant 2,

K1 = calibration constant 1, and

L = spectral radiance.

Finally, convert the BT in Kelvin degrees to Celsius degrees using the following formula:

$$\mathrm{C(LST)} = T(\mathrm{BT}) - 273.15. \quad (9)$$

(ii) GIS digitizing: The aerial photographs from 1995 to 2021 found on Geomolg [23] have been used to define the urban built-up areas. The built-up areas in this research refer to the boundaries of existing buildings within the administrative boundaries of each community. These built-up areas were manually drawn using GIS ArcMap. After drawing them, they were extracted from the administrative boundaries to find the open areas for each city (un-built areas).

(iii) GIS modeling: Contour lines have been used to find the topography of all places in the West Bank. The topography of the West Bank was prepared by applying the GIS tool "topo to raster" to a contour shape file.

Step #3: Relational analysis: Correlation analysis was used to find the relationship between the topography of each region with LST and built-up or un-built areas and LST. The correlation coefficient was used to study this relationship to show if the correlation relationship is positive or negative and ranges between +1 and −1. The positive value indicates a direct relationship between the studied raster images, while the negative value indicates a negative relationship. The tool used in this study to find this index is "Band Collection Statistics." This tool provides statistics for the multivariate analysis of the studied raster images. It also offers matrices for the covariance and correlation of the studied raster images. One of the matrices includes each raster's minimum value, maximum value, mean, and standard deviation. Another matrix is the correlation matrix, which shows the correlation coefficient values (correlation indices) that indicate the relationship between the studied raster images. The indices from this matrix are built by relating the value of each cell of the first raster with the value of the same cell from the second raster. Therefore, the correlation between the raster images is a measure of dependency between them. The equation to calculate the correlation [27] is as follows:

$$\mathrm{Corr(ij)} = \mathrm{Cov(ij)}/\sigma i \times \sigma j, \quad (10)$$

where Corr($ij$) is the correlation index between the studied rasters, Cov($ij$) is the covariance between them, and $\sigma i$ and $\sigma j$ are the standard deviations of them.

For this step, only the areas covered by the studied communities were analyzed because the land cover raster has places with no data. So, the LST raster was clipped to show the boundaries of the communities. The same cell size was used for both rasters.

## 4. Results and Discussion

The developed methodological framework was applied for the 10 studied cities in the West Bank, and the results of the correlated analysis between built-up area, land cover, and soil with LST are shown below.

### *4.1. The Relationship between Land Cover and LST*

*4.1.1. Built-Up Area (Continuous and Discontinuous Urban Fabric).* The 10 selected cities' built-up areas are rapidly expanding and becoming denser mainly because of Israeli occupation policies, which prevented Palestinian development in areas classified as C according to the Oslo Agreement, where there is no Palestinian control. Due to the former, rapid growth in areas classified as A and B, which constituted only 21% of the West Bank, was far more noticeable. This, in turn, explains the highly dense built-up area and the disappearance of agricultural lands in these areas over the last 26 years. Urban sprawl stretched the boundaries of the urban spaces, linking these cities and refugee camps with neighboring towns and villages. This merging led to the birth of large-scale urban areas with unrecognizable boundaries, forming big cities [28] (Figure 3).

The West Bank GIS maps illustrate the changes in the built-up area. It was noticed that the change in the area was different in each of the 10 cities. Table 4 illustrates the built-up area in the 10 cities compared to their administrative area in the years 1995–2021. The table was obtained from aerial photos of the West Bank from the years studied by digitizing the built-up area for each community and measuring the areas. Then, Table 5 and Figure 4 explain the growth rate percentage in the built-up area.

As indicated in Table 6, Jenin's built-up area showed the highest increase among the 10 cities in the year 2021, with an increase of 2.99 $km^2$ from 2015 to 2021; however, Tubas showed the highest increase in built-up area of 2.96 $km^2$ between the years 2005 and 2010. Moreover, Bethlehem's built-up area did not show an increase between the years 1995–2021. In addition to the latter, Hebron did not show an increase between the years 2000–2021. The expansion of these two cities was limited due to the Israeli occupation's spatial constraints; the Israeli Separation wall encloses Bethlehem, while illegal Israeli settlements surround Hebron, and most of its land is classified as area C. Thus, both cities used the infill (highly dense built-up area) approach as a solution for development, and this increase in built-up area impacted the LST for these cities.

*4.1.2. Land Surface Temperatures (LST).* Figure 5 shows LST for the West Bank in the summer, particularly August, during the years 1995–2021. The figure explains how the LST values varied over the years but without a defined pattern. The highest values of LST peaked in the year 2005 (70.44°)


FIGURE 3: Urban sprawl: expansion of the built-up area for the 10 main cities (map prepared by researchers, dataset source: MoLG (Ministry of Local Government) [23]).

TABLE 4: Built-up area in km$^2$ between 1995 and 2021.

| City | Administrative area in km$^2$ | Built-up area in km$^2$ | | | | | |
|---|---|---|---|---|---|---|---|
| | | 1995 | 2000 | 2005 | 2010 | 2015 | 2021 |
| Jenin | 39.461 | 5.964 | 6.065 | 7.065 | 9.066 | 10.566 | 13.556 |
| Qalqilia | 10.252 | 2.371 | 3.292 | 4.542 | 5.542 | 6.542 | 7.347 |
| Salfit | 22.663 | 2.101 | 3.190 | 4.440 | 4.540 | 4.690 | 5.440 |
| Nablus | 32.404 | 13.100 | 14.062 | 15.312 | 15.705 | 17.205 | 17.755 |
| Tubas | 223.123 | 1.001 | 1.946 | 3.196 | 6.160 | 7.660 | 8.660 |
| Jericho | 172.048 | 5.451 | 5.726 | 6.976 | 7.726 | 8.476 | 9.476 |
| Bethlehem | 10.608 | 5.580 | 5.580 | 5.580 | 5.580 | 5.580 | 5.580 |
| Ramallah and Al-Bireh | 17.671 | 15.406 | 17.306 | 17.805 | 18.103 | 18.452 | 18.727 |
| Tulkarem | 20.486 | 2.175 | 3.224 | 4.224 | 6.136 | 7.136 | 8.136 |
| Hebron | 46.160 | 24.712 | 46.161 | 46.161 | 46.161 | 46.161 | 46.161 |

TABLE 5: Growth in built-up area between 1995 and 2021.

| City name | Growth in built-up area | | | | |
|---|---|---|---|---|---|
| | 2000–1995 (%) | 2005–2000 (%) | 2010–2005 (%) | 2015–2010 (%) | 2021–2015 (%) |
| Jenin | 2 | 16 | 28 | 17 | 28 |
| Qalqilia | 39 | 38 | 22 | 18 | 12 |
| Salfit | 52 | 39 | 28 | 33 | 16 |
| Nablus | 7 | 9 | 3 | 10 | 3 |
| Tubas | 94 | 64 | 93 | 24 | 13 |
| Jericho | 5 | 22 | 11 | 10 | 12 |
| Bethlehem | 0 | 0 | 0 | 0 | 0 |
| Ramallah and Al-Bireh | 12 | 3 | 2 | 2 | 1 |
| Tulkarem | 48 | 31 | 45 | 16 | 14 |
| Hebron | 87 | 0 | 0 | 0 | 0 |

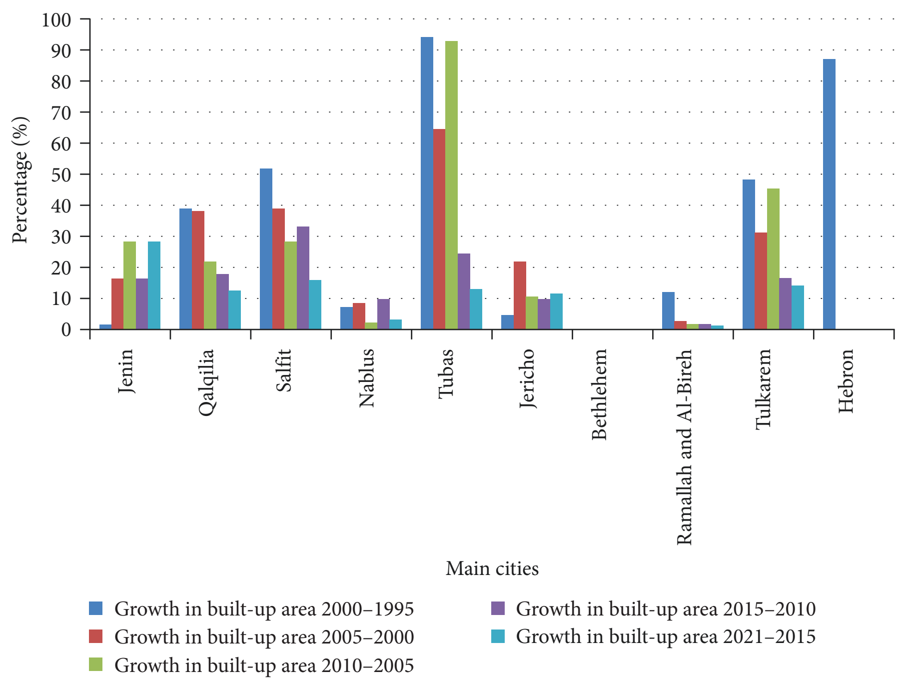


FIGURE 4: Growth in built-up area between 1995 and 2021 for the 10 main cities (source: researchers).

TABLE 6: Annual change in buildings area and built-up area in $km^2$ during the study period 1995–2021, (source: MoLG (Ministry of Local Government) [23]).

| City | Buildings ($km^2$) | Built-up area ($km^2$) |
|---|---|---|
| Jenin | 0.028 | 0.296 |
| Qalqilia | 0.029 | 0.191 |
| Salfit | 0.006 | 0.073 |
| Nablus | 0.082 | 0.233 |
| Tubas | 0.013 | 0.295 |
| Jericho | 0.009 | 0.232 |
| Bethlehem | 0.014 | 0.000 |
| Ramallah and Al-Bireh | 0.050 | 0.192 |
| Tulkarem | 0.033 | 0.299 |
| Hebron | 0.127 | 0.825 |

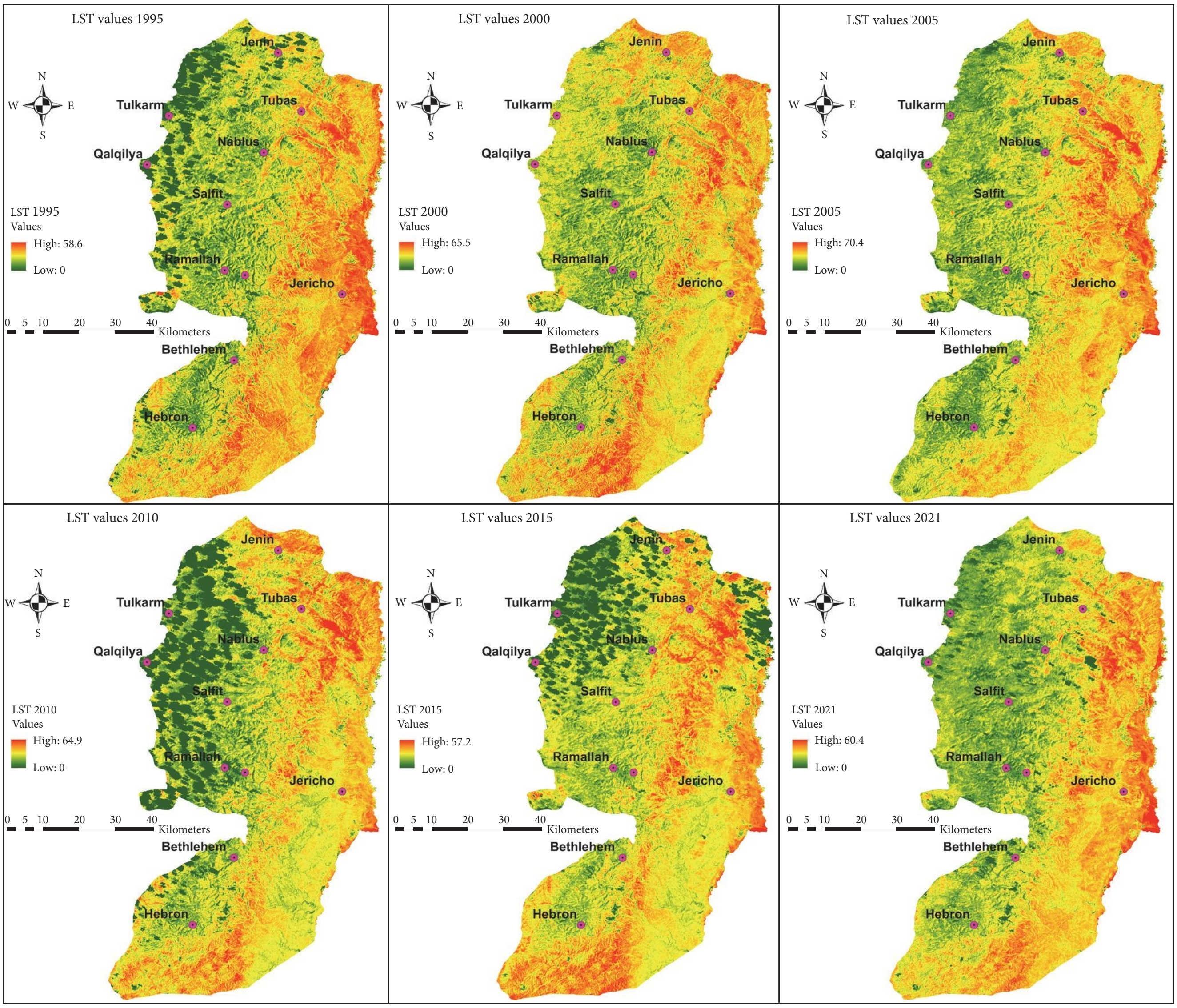


Figure 5: LST (Celsius) for the West Bank in summer (August) during the years 1995–2021 (map prepared by researchers, dataset source: RM–LANDSAT).

and had the lowest value (57.26°) in 2015. However, these values do not mean the land surface was warmer in 2005 than in other years. The most frequent values during the years were 40° in 1995, 50° in 2000, 52° in 2005, 44° in 2010, 41° in 2015, and 46° in 2015. This means that the years 2000 and 2005 can be described as the warmest years (Table 7). These frequent values were found in the statistics charts of LST values.

Tables 8 and 9 and Figure 6 summarize the highest (maximum) LST values for each year for the 10 studied cities in this paper. Furthermore, it also shows the trend of LST for each city over the study period. Notably, the values were higher during the years 2000 and 2005 than in the other years. Studying each city, results show that Jenin in 2000 and Tubas in 2005 had the highest temperature values among the other cities in the West Bank. Tubas has the highest temperature values in 2005, 2010, and 2020. Meanwhile, Ramallah and Al-Bireh, Bethlehem, and Hebron had moderate temperature values, with the highest temperature in Ramallah being 54.2° in 2000, Bethlehem at 54.4°, and Hebron at 57.9°. Moreover, Salfit, Tulkarem, and Qalqilia had low-temperature values among the other cities during the years 1995–2021.

Comparing the LST of each city between the years as shown in Table 10 shows the differences between LST values of each of

Table 7: Frequent temperatures for each year in the West Bank in Celsius degrees.

| Year | Temperature WB |
|---|---|
| 1995 | 39° and 46° |
| 2000 | From 48° to 53° |
| 2005 | From 50° to 53° |
| 2010 | 48° |
| 2015 | 44° |
| 2021 | 43° and 49° |

Table 8: Highest temperature value in Celsius degrees for each city in each studied year.

| City name | 1995 | 2000 | 2005 | 2010 | 2015 | 2021 |
|---|---|---|---|---|---|---|
| Jenin | 49.4 | 61.9 | 58.4 | 58.7 | 50.2 | 50.6 |
| Qalqilia | 45.8 | 55.2 | 52.9 | 48.4 | 46.8 | 47.2 |
| Salfit | 44.5 | 52.1 | 53.9 | 52.1 | 48.1 | 45.9 |
| Nablus | 51.7 | 58.6 | 61.4 | 58.7 | 54.5 | 54.1 |
| Tubas | 52.3 | 60.3 | 61.9 | 58.7 | 53.2 | 54.9 |
| Jericho | 53.5 | 58.9 | 59.9 | 57.5 | 51.2 | 54.7 |
| Bethlehem | 47.0 | 55.2 | 54.4 | 52.1 | 47.8 | 50.2 |
| Ramallah and Al-Bireh | 46.4 | 54.2 | 53.9 | 51.5 | 47.2 | 47.5 |
| Tulkarem | 47.6 | 56.6 | 52.9 | 50.9 | 43.5 | 47.6 |
| Hebron | 47.6 | 57.9 | 56.9 | 54.5 | 49.4 | 51.4 |

Table 9: Cities with the highest and lowest temperatures in Celsius degrees in each studied year.

| | 1995 | 2000 | 2005 | 2010 | 2015 | 2021 |
|---|---|---|---|---|---|---|
| Highest temperature value | 53.5 (Jericho) | 61.9 (Jenin) | 61.9 (Tubas) | 58.7 (Tubas) | 54.5 (Nablus) | 54.9 (Tubas) |
| Lowest temperature value | 45.8 (Qalqilia) | 52.1 (Salfit) | 52.9 (Tulkarem) | 48.4 (Qalqilia) | 43.5 (Tulkarem) | 45.9 (Salfit) |

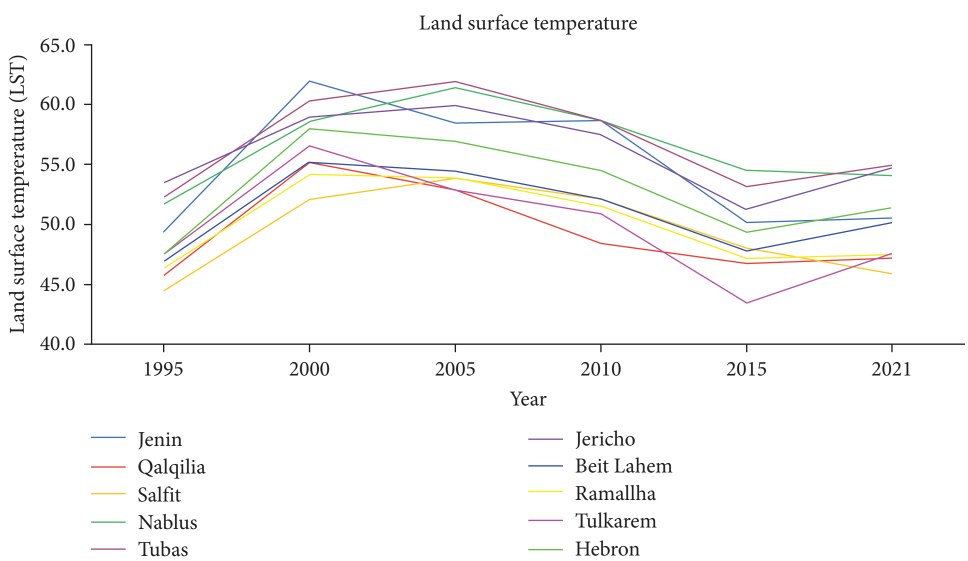


Figure 6: Line graph of highest temperature value in Celsius degrees for each city in each studied year.

the two studied periods; the difference between the years 1995 and 2000 is positive as the temperature increased for all of the cities and is notable and did not occur afterward. Jenin faced the highest increase with 12.5°, Hebron faced the second highest increase with 10.3°, and Jericho had the lowest increase, which was 5.4°. Between the years 2000 and 2005, LST decreased for all of the cities. Nevertheless, Salfit, Nablus, Tubas, and Jericho's temperatures were positive and higher. Between the years 2010 and 2015, the LST had decreased in all the studied cities. Jenin had the highest decrease in temperature, while Qalqilia had the lowest decrease. After that, between the years 2015 and 2021, only Salfit and Nablus cities faced a decline in the LST, while other cities faced an increase in LST.

*4.1.3. Correlation Analysis between Built-Up Area and LST.* The applied methodology of using GIS (band collection statistics) in Table 11 shows the correlation indices for each year between the LST values and the built-up area for the whole West Bank. Analysis was done of the built-up areas of the 10 cities in the West Bank in relation to the LST. Results found a negative correlation between the built-up area for said cities and the LST. It was also found that the correlation indices were negative for all years except in the year 2015, which was positive. This means that there is an inverse relationship between built-up area and LST. We found that this result is similar to what Bonafoni and Keeratikasikorn [12] argued: LST decreases as the albedo of the built-up surface increases.

Table 10: LST difference between studied years (in Celsius degrees).

| City name | 1995–2000 | 2000–2005 | 2005–2010 | 2010–2015 | 2015–2021 |
|---|---|---|---|---|---|
| Jenin | 12.5 | −3.5 | 0.2 | −8.5 | 0.4 |
| Qalqilia | 9.4 | −2.3 | −4.5 | −1.6 | 0.4 |
| Salfit | 7.5 | 1.8 | −1.8 | −4.0 | −2.2 |
| Nablus | 6.8 | 2.8 | −2.7 | −4.2 | −0.4 |
| Tubas | 8.0 | 1.6 | −3.2 | −5.5 | 1.7 |
| Jericho | 5.4 | 1.0 | −2.5 | −6.2 | 3.5 |
| Bethlehem | 8.2 | −0.8 | −2.3 | −4.3 | 2.4 |
| Ramallah and Al-Bireh | 7.8 | −0.3 | −2.4 | −4.3 | 0.3 |
| Tulkarem | 9.0 | −3.7 | −2.0 | −7.4 | 4.1 |
| Hebron | 10.3 | −1.0 | −2.4 | −5.1 | 2.0 |

Table 11: Correlation indices for each year between LST and built-up areas.

| Year | Correlation coefficient | Highest value of LST (Celsius degrees) |
|---|---|---|
| 1995 | −0.03851 | 58.59 |
| 2000 | −0.03777 | 66.50 |
| 2005 | −0.04104 | 70.44 |
| 2010 | −0.05372 | 69.46 |
| 2015 | 0.00425 | 59.46 |
| 2021 | −0.04133 | 60.42 |

*4.2. Land Cover 2021.* In the studied regions for the year 2021, land cover has changed, thus affecting environmental implications and urbanization. By comparing the LST map (Figure 7) with the land cover map (Figure 8) for the West Bank for the year 2021, it is found that the highest LSTs in the West Bank are concentrated to the east, as shown in Figure 7. The land cover in these areas is either bare land or grassland. Moreover, the relationship between this kind of land cover (open spaces) and high degrees of LST means that LST increases in places with no shade. On the other hand, the LST decreases when moving from the east to the west of the West Bank. This decrease can be explained by the land cover, which is either shrubland, cropland, tree cover, or built-up area. This proves that changes in land cover (surface properties and vegetation presence) in urban areas can effectively modify the near-surface local climate. LST decreases as the albedo of the built-up surface increases. If we compare the built-up area in the West Bank and the open area surrounding it, we can see that the LST for the built-up area is less than that of the open area outside. This is due to the fact that the land cover in this area is either bare, grass, or cropland, and as previously indicated, this kind of land cover does not provide shade. However, in shrublands, land with tree cover, and built-up areas, LST is lower because of the existing shade. Thus, the more shade the land cover or land use makes, the less LST. Therefore, in the case of the built-up area, this indicates that the denser the built-up area, the less the LST, the higher the natural temperatures, and thus, the lesser environmental quality and live comfort quality.

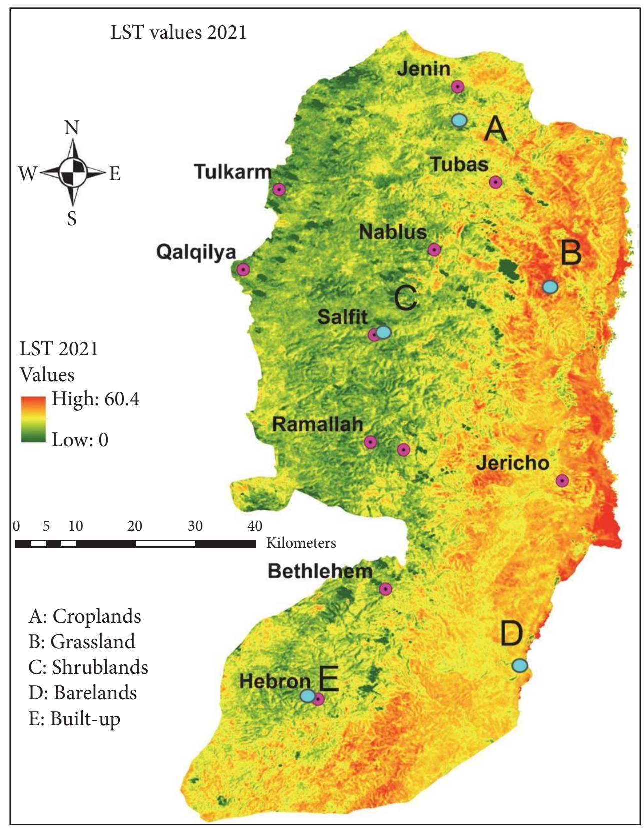


Figure 7: Overlap for some locations between LST in 2021 and land cover.

Figure 9 illustrates the built-up areas and open spaces (outside the built-up areas) in three cities, Jenin, Tubas, and Salfit, as examples of different temperature rates. It is noticed that Tubas has high LST values, Jenin has moderate LST values, and Salfit has low LST values. It can be seen that LST values are higher in open spaces than in built-up areas within the boundaries of all three cities. Most open spaces are covered by cropland in Jenin, grassland in Tubas, and shrubland in Salfit. This explains the high LST for the built area compared to the surrounding open spaces.

*4.2.1. Correlation Analysis between Land Cover 2021 and LST.* To understand this change for the cities with the highest and

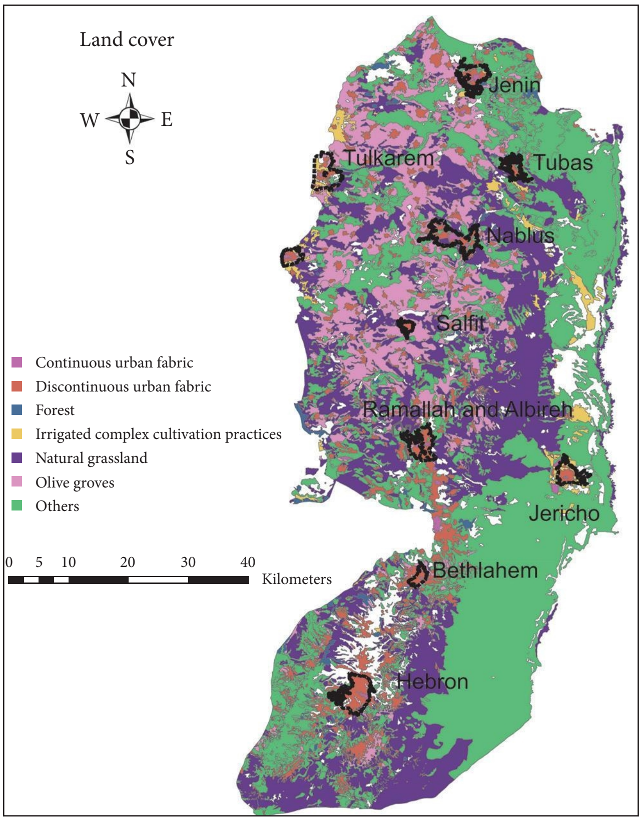


FIGURE 8: Land cover map of West Bank 2021 (ESA world cover project 2021).

lowest temperature values for LST, we checked the relation between LST and land cover for each city. Table 12 shows the land cover for the cities—with the highest and lowest LST as indicated in Table 9 and the LST value for each city's land cover. Their land cover is categorized into six classes: continuous and discontinuous urban fabric, olives groves, natural grassland, forest, and irrigated complex cultivation practices. For the land cover, olives groves, natural grassland, forest, and irrigated complex cultivation practices, natural grassland does not make shade on the ground. Thus, it affects LST in high value; olive trees create shade and less LST, but the forest makes the lowest LST value for its density.

However, our results were opposite to those of Ayanlade et al. [4], who argued that the loss in the vegetal cover encouraged an increase in the built-up area. He also claimed that cities' high density of built-up areas witnessed higher LST compared with the open area surrounding them. Our results indicated that different land cover types of the dense urban area of the 10 cities affected the spatial pattern of urban LST. In addition, the distribution of LST intensity in the urban area depends on changes in land cover.

*4.3. The Relationship between Soil Type and LST (in Celsius Degrees).* West Bank's soil type varies from the eastern to western areas in vertical slats, as illustrated in Figure 10. From the east to west, these types are regosols and bare rocks, loessial serozems, brown lithosols, brown rindzinas, and terra rossas. By comparing the distribution of these types with the LST values of the West Bank, we can notice that LST values have the highest values in the eastern areas and decrease when we go to the west. This LST value distribution throughout the years is similar to the vertical distribution of soil types from east to west. This, in turn, indicates that the soil type dramatically affects the LST values. Redosols, loessial serozems, brown lithosols, and rindzinas are brown and red soils with clay layers, causing the land to absorb the sun's radiation. This relationship between soil type and LST, however, is also affected by land cover. From Tables 12 and 13, for example, in Jericho, the soil type is regosols and loessial, with the highest LST values of 51.25° and 49.37°, respectively. However, the continuous and discontinuous urban fabric areas on these two soil types have 48.5° of LST values. This, in turn, leads us to the fact that these land cover types that shade over the land lead to a decrease in temperatures. From Table 13, regosols and loessial types have the highest values and are only available in Jericho. On the other hand, Qalqilia, Salfit, and Tulkarem have grumusols, terra Rossa, or brown rendzinas types only, making their LST values medium or low.

Table 14 explains the relationship between land cover, soil, and LST and how land cover and soil type play a role in changing and affecting LST value. In this table, we focused on the built-up areas and their surroundings in six cities: Jericho, Jenin, Tubas, Nablus, Qalqilia, and Salfit. This explains how built-up areas have lower LST than their surroundings due to the impact of shade and shadows of the building, while in their surroundings, the land cover is an open area with grass and vegetation. Thus, soil type plays a noticeable role in the aforementioned area as it is unbuilt. This also confirms how soil is important in changing LST when land cover is unbuilt.

## 5. Conclusion

The results of this paper showed that the expansion and increase of the built-up area, changing land cover, and different soil types in the 10 major cities in the West Bank led to a change in LST. The developed methodological framework using GIS and RS explained an inverse relationship between land cover, soil, and LST. Furthermore, there is a positive and direct relationship between LST in the studied cities of the region in the years between 1995 and 2021.

(i) For the built-up area, the negative correlation between LST and built-up area contravenes our hypothesis of a positive correlation between LST and built-up areas. In 2021, it was found that the highest LSTs in the West Bank are concentrated to the east of the region, while the LST decreases when moving to the west.

(ii) Moreover, it is found that LST decreases as the albedo of the built-up surface increases. We assume that this unexpected result is because of the change in the land cover and land use around built-up areas, for most land cover around the built-up area is open space covered by cropland. This is clear in the six

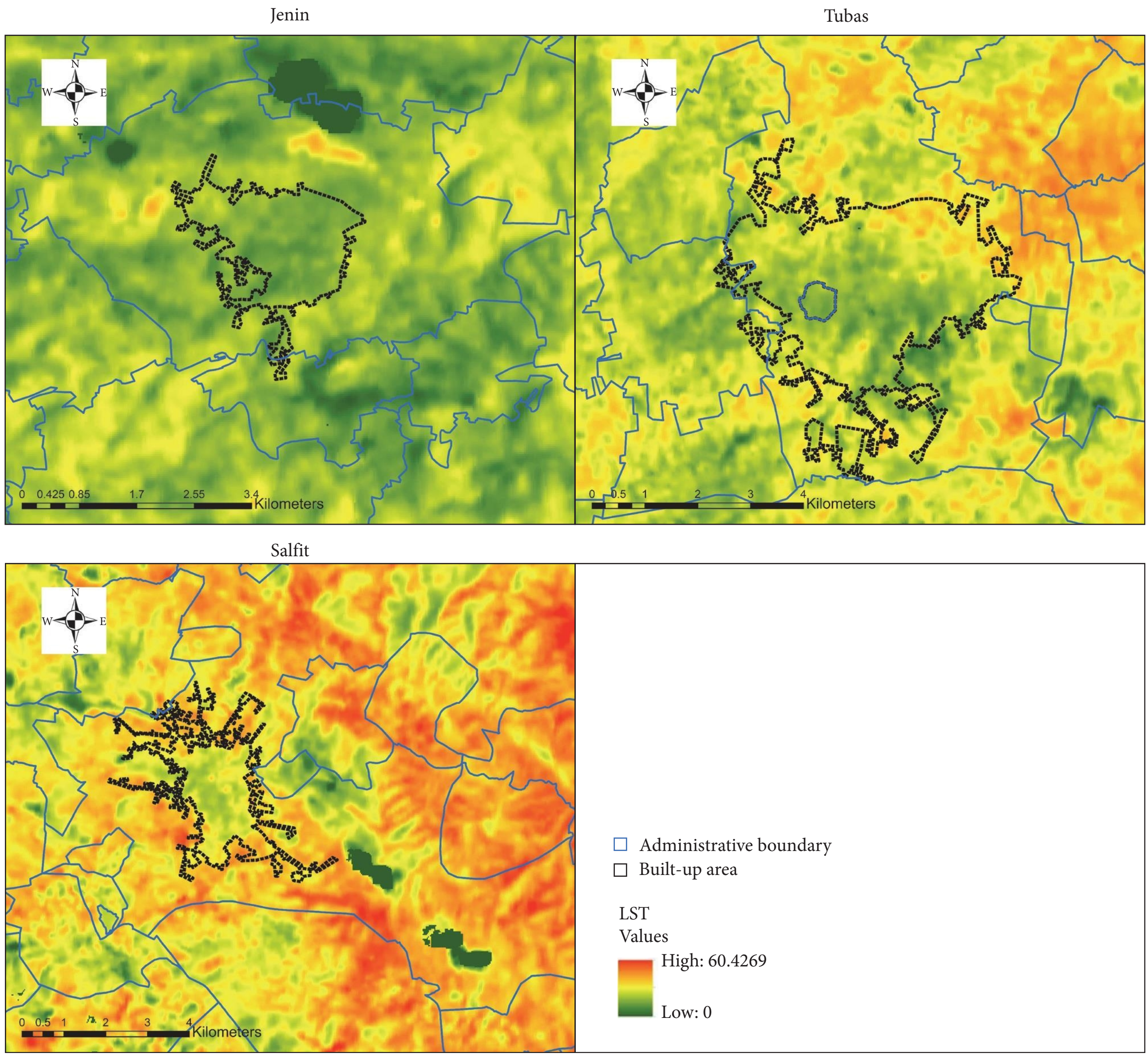


FIGURE 9: Overlap for some locations between LST (in Celsius degrees) in 2021 and land cover.

cities we chose to explain the relation between LST, built-up areas, and open spaces, as seen in Jenin. LST is considered moderate for open spaces classified as grassland in Tubas, while LST is considered high for open spaces in that same city. Moreover, it is considered low for open space classified shrubland in Salfit. This is due to the fact that this kind of land cover does not make shade on the ground.

(iii) Due to the former, it is concluded that this is the reason for the LST increase in these areas, while LST decreased in the built-up area because of the shade the buildings project and the soil type that plays a considerable role. Thus, we find that the more shade the land cover or land use makes, the less the LST, whereas in cases where the land cover is unbuilt, and the space is open, the type of soil is the factor that plays a significant role in changing LST. It is worth mentioning that in the West Bank, the soil type varies from east to west, causing higher LST as one moves from east to west.

These results help municipalities and urban planners in Palestine to understand the impact, processes, and consequences of changing built-up areas and land use on LST. Moreover, it will assist them in thinking about cities in a sustainable way to stop unplanned cities' expansion, which in turn leads to urban sprawl. Furthermore, it should help them to think about future master plans and proposed land uses. The methodological framework used in this paper can help in future comparison studies. The band collection statistics tool helps study the correlation between different information for the exact location.

Table 12: LST for the difference land cover for selected cities.

| City | Discontinuous urban fabric | | Olive groves | | Natural grassland | | Irrigated complex cultivation practices | | Forest | | Continuous urban fabric | |
|---|---|---|---|---|---|---|---|---|---|---|---|---|
| | LST value | Area ($km^2$) | LST value | Area ($km^2$) | LST value | Area ($m^2$) | LST value | Area ($km^2$) | LST value | Area ($km^2$) | LST value | Area ($km^2$) |
| Jenin | 43.78 | 5.53 | 45.16 | 0.7619 | 43.41 | 0.54 | 45.09 | 0.421 | 42.98 | 0.3400 | 42.14 | 1.184 |
| Qalqilia | 41.01 | 2.80 | 42.87 | 0.6683 | 44.57 | 0.07 | 41.85 | — | — | 0.0000 | 40.86 | 0.668 |
| Salfit | 42.26 | 2.36 | 43.14 | 0.6250 | 44.60 | 0.03 | — | — | 41.30 | 0.0022 | — | 0.000 |
| Nablus | 42.81 | 10.19 | 42.04 | 1.5214 | 45.27 | 3.96 | — | — | 45.74 | 0.2901 | 42.21 | 2.069 |
| Tubas | 45.39 | 2.36 | 47.05 | 0.3431 | 48.66 | 0.41 | 48.65 | 0.083 | 44.47 | 0.0230 | — | 0.000 |
| Jericho | 48.57 | 6.18 | — | 0.0000 | — | 0.00 | 49.95 | 4.181 | — | 0.0000 | 48.51 | 0.232 |
| Tulkarem | 37.30 | 6.71 | 33.70 | 2.3436 | 44.41 | 1.21 | 40.44 | 4.607 | 41.66 | 0.0025 | 39.94 | 0.420 |

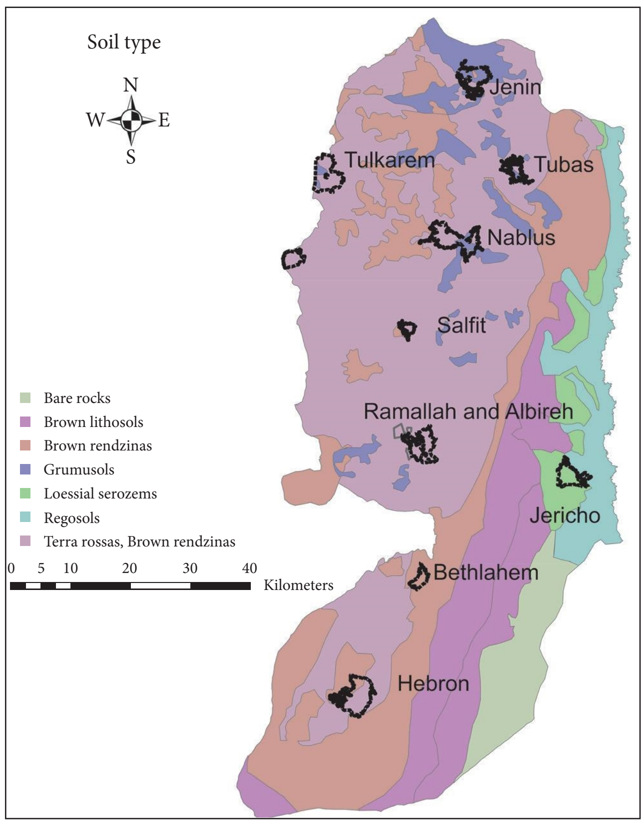


Figure 10: West Bank's soil type.

Table 13: LST for the difference soil for selected cities (in Celsius degrees).

| City name | Soil type | | | | |
|---|---|---|---|---|---|
| | Grumusols | Terra rossas, brown rendzinas, and pale rendzinas | Brown rendzinas and pale renzinas | Loessial serozems | Regosols |
| Jenin | 45.421691 | 44.897172 | 43.135886 | — | — |
| Qalqilia | — | 42.152461 | — | — | — |
| Salfit | — | 42.996774 | 42.790756 | — | — |
| Nablus | 46.18553 | 43.425112 | 42.796735 | — | — |
| Tubas | 47.338568 | 47.398834 | — | — | — |
| Jericho | — | — | — | 49.377619 | 51.252128 |
| Tulkarem | 41.78235 | 37.986909 | — | — | — |

Table 14: The relationship between land cover, soil type, and LST.

| Community | Land cover | Soil type |
|---|---|---|
| Jericho | 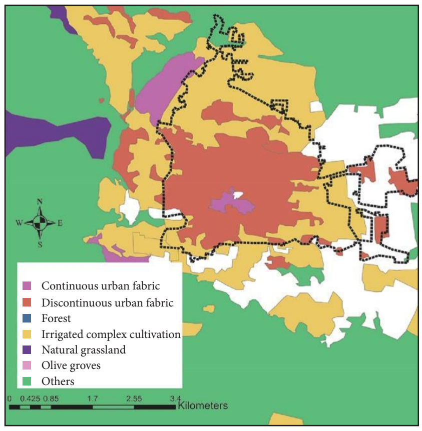 | 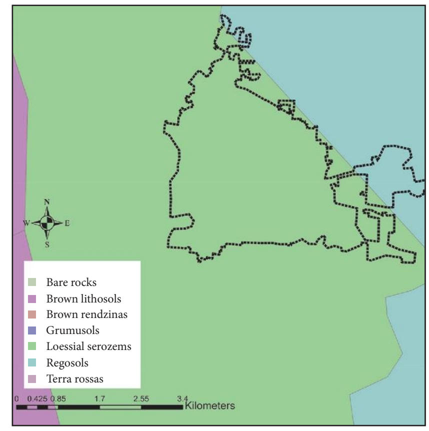 |
| Jenin | 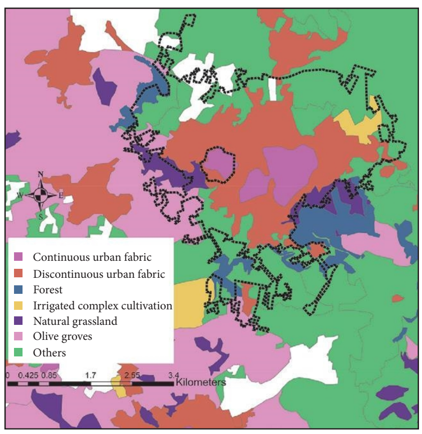 | 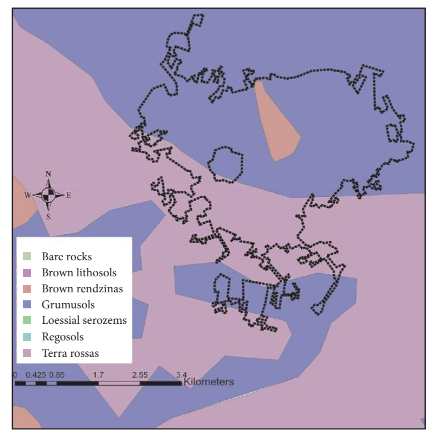 |
| Tubas | 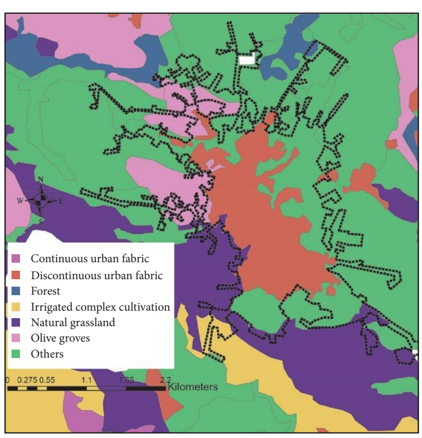 | 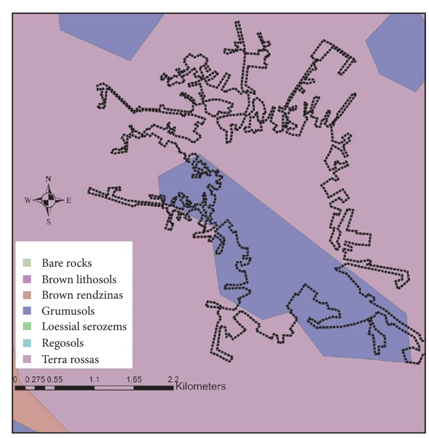 |
| Nablus | 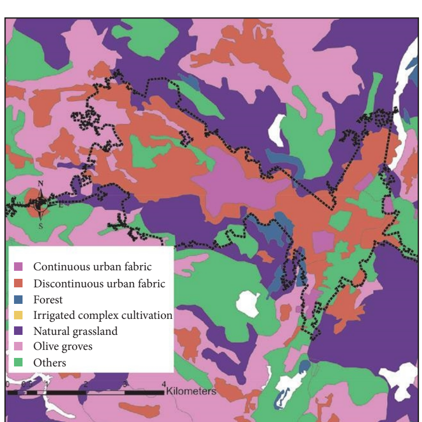 | 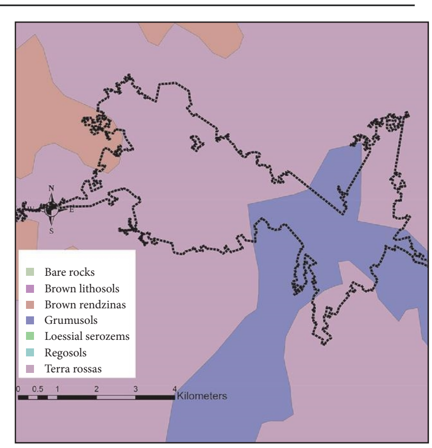 |

The paper faced some limitations, such as being unable to obtain the mean values for LST for West Bank, Palestine, because the LST values have been affected by clouds, which makes the value zero very regular, thus making the mean value not helpful or even correct. Moreover, the authors found difficulties in obtaining images for LULC during the whole study period, and only LULC images for the year 2021 are available through the national Geomolg website [23]. Obtaining images for the WB for LULC from the American website was complex.

## Data Availability

Data will be available on request through the authors themselves (contacted person is Zahraa Zawawi; email: zahraa.zawawi@najah.edu; An-Najah National Univeristy, Nablus, Palestine).

## Conflicts of Interest

The authors declare that they have no conflicts of interest.

## References

[1] J. N. ObiefuNa, C. J. OkOlie, P. C. NwilO, O. E. Daramola, and L. C. Isiofia, "Potential influence of urban sprawl and changing land surface temperature on outdoor thermal comfort in Lagos State, Nigeria," *Quaestiones Geographicae*, vol. 40, no. 1, pp. 5–23, 2021.

[2] J. N. Obiefuna, P. C. Nwilo, C. J. Okolie, E. I. Emmanuel, and O. E. Daramola, "Dynamics of land surface temperature in response to land cover changes in Lagos metropolis," *Nigerian Journal of Environmental Sciences and Technology*, vol. 2, no. 2, pp. 148–159, 2018.

[3] A-A. Kafy, A.-A. Faisal, A. Al Rakib et al., "Predicting changes in land use/land cover and seasonal land surface temperature using multi-temporal landsat images in the northwest region of Bangladesh," *Heliyon*, vol. 7, no. 7, Article ID e07623, 2021.

[4] A. Ayanlade, M. I. Aigbiremolen, and O. R. Oladosu, "Variations in urban land surface temperature intensity over four cities in different ecological zones," *Scientific Reports*, vol. 11, no. 1, pp. 1–17, 2021.

[5] A. Maishella, B. E. B. Dewantoro, and M. A. P. Aji, "Correlation analysis of urban development and land surface temperature using google earth engine in sleman regency, Indonesia," in *IOP Conference Series: Earth and Environmental Science*, IOP Publishing, Article ID 012018, 2020.

[6] A. G. C. Ovalle, A. C. Tristán, J. A. Amador-Nieto, R. F. Putri, and R. A. Zahra, "Analysing the land use/land cover influence on land surface temperature in San Luis Potosí Basin, México using remote sensing techniques," *IOP Conference Series: Earth and Environmental Science*, vol. 686, Article ID 012029, 2021.

[7] A. A. Bindajam, J. Mallick, S. AlQadhi, C. K. Singh, and H. T. Hang, "Impacts of vegetation and topography on land surface temperature variability over the semi-arid mountain cities of Saudi Arabia," *Atmosphere*, vol. 11, no. 7, Article ID 762, 2020.

[8] J. He, W. Zhao, A. Li, F. Wen, and D. Yu, "The impact of the terrain effect on land surface temperature variation based on Landsat-8 observations in mountainous areas," *International Journal of Remote Sensing*, vol. 40, no. 5-6, pp. 1808–1827, 2018.

[9] J. Song, W. Chen, J. Zhang, K. Huang, B. Hou, and A. V. Prishchepov, "Effects of building density on land surface temperature in China: spatial patterns and determinants," *Landscape and Urban Planning*, vol. 198, Article ID 103794, 2020.

[10] M. S. Asyraf, A. Damayanti, and M. Dimyati, "The effect of building density on land surface temperature, (Case Study: Turikale District, Maros Regency)," in *IOP Conference Series: Earth and Environmental Science*, IOP Publishing, Article ID 012061, 2020.

[11] V. M. Sayão, N. V. dos Santos, W. de Sousa Mendes et al., "Land use/land cover changes and bare soil surface temperature monitoring in southeast Brazil," *Geoderma Regional*, vol. 22, Article ID e00313, 2020.

[12] S. Bonafoni and C. Keeratikasikorn, "Land surface temperature and urban density: multiyear modeling and relationship analysis using MODIS and Landsat data," *Remote Sensing*, vol. 10, no. 9, Article ID 1471, 2018.

[13] X. Peng, W. Wu, Y. Zheng, J. Sun, T. Hu, and P. Wang, "Correlation analysis of land surface temperature and topographic elements in Hangzhou, China," *Scientific Reports*, vol. 10, no. 1, pp. 1–16, 2020.

[14] M. Yasir, S. Hui, S. U. Rahman, M. Ilyas, A. Zafar, and A. Mehmood, "Estimation of land surface temperature using LANDSAT-8 data-A case study of district Malakand, Khyber Pakhtunkhwa, Pakistan," *Journal of Liberal Arts and Humanities*, vol. 1, pp. 140–148, 2020.

[15] Y. Xue, H. Lu, Y. Guan, P. Tian, and T. Yao, "Impact of thermal condition on vegetation feedback under greening trend of China," *Science of the Total Environment*, vol. 785, Article ID 147380, 2021.

[16] I. Rousta, H. Olafsson, M. H. Nasserzadeh, H. Zhang, J. Krzyszczak, and P. Baranowski, "Dynamics of daytime land surface temperature (LST) variabilities in the Middle East countries during 2001–2018," *Pure and Applied Geophysics*, vol. 178, no. 6, pp. 2357–2377, 2021.

[17] X.-L. Chen, H.-M. Zhao, P.-X. Li, and Z.-Y. Yin, "Remote sensing image-based analysis of the relationship between urban heat island and land use/cover changes," *Remote Sensing of Environment*, vol. 104, no. 2, pp. 133–146, 2006.

[18] T. Das and S. Das, "Analysing the role of land use and land cover changes in increasing urban heat phenomenon in Chandannagar city, West Bengal, India," *Journal of Earth System Science*, vol. 131, no. 4, Article ID 261, 2022.

[19] S. R. Aldhshan and H. Z. M. Shafri, "Change detection on land use/land cover and land surface temperature using spatiotemporal data of Landsat: a case study of Gaza Strip," *Arabian Journal of Geosciences*, vol. 12, no. 14, pp. 1–14, 2019.

[20] A. Ghodieh, "Urban built-up area estimation and change detection of the occupied West Bank, Palestine, using multi-temporal aerial photographs and satellite images," *Journal of the Indian Society of Remote Sensing*, vol. 48, no. 2, pp. 235–247, 2020.

[21] S. Raddad, "Assessing land use/cover changes under political transitions using remote sensing and geographic information systems," *International Journal of Environment, Society and Space*, vol. 3, no. 1, pp. 57–68, 2015, 2015.

[22] Palestinian Central Bureau of Statistics (PCBS), "Population in Palestine 2022," 2022.

[23] MoLG (Ministry of Local Government), "Geomolg: integrated spatial information system in Palestine," 2022.

[24] U.S. Geological Survey (USGS), "Earth explorer," 2022, Accessed June 10, 2022, https://earthexplorer.usgs.gov/.

[25] Y. Sun, “Retrieval and application of land surface temperature,” *Geo. Utexas. Edu*, vol. 1, no. 1, pp. 1–27, 2008.
[26] J. Oppong, “How to use ArcGIS pro to calculate land surface temperature (LST) from Landsat imagery,” 2021, Accessed Sep 2022, https://www.gislounge.com/how-to-use-arcgis-pro-to-calculate-land-surface-temperature-lst-from-landsat-imagery/.
[27] Esri, “How Band Collection Statistics works,” accessed 20 August 2022, https://pro.arcgis.com/en/pro-app/latest/tool-reference/spatial-analyst/how-band-collection-statistics-works.htm.
[28] World Bank Blog, “Connecting Palestinian cities for a more sustainable future,” 2017, Retrieved December 20, 2022, from https://blogs.worldbank.org/arabvoices/connecting-palestinian-cities-more-sustainable-future.